0026-895X/01/6002-331–340$3.00
MOLECULAR PHARMACOLOGY
Copyright © 2001 The American Society for Pharmacology and Experimental Therapeutics
*Mol Pharmacol* 60:331–340, 2001

Vol. 60, No. 2
839/921712
*Printed in U.S.A.*



# δ-Opioid Receptor Gene: Effect of Sp1 Factor on Transcriptional Regulation in Vivo

DMITRI SMIRNOV, HEE-JEONG IM, and HORACE H. LOH

*Department of Pharmacology, University of Minnesota Medical School, Minneapolis, Minnesota*

Received January 24, 2001; accepted May 14, 2001

This paper is available online at http://molpharm.aspetjournals.org

## ABSTRACT

δ-Opioid receptor (DOR) promoter exhibited a cell-type–specific expression pattern. Protein-DNA interactions in this promoter were identified by dimethyl sulfate in vivo footprinting analysis of NG108-15 cells, expressing endogenous DOR. Complete protection of the putative Sp1 *cis*-element and partial protection of the sequence defined as X-*Not*I in the basal promoter were observed only in the $G_0/G_1$ phase of the cell cycle. No protection was detected in Neuro2A cells that do not express DOR. In vivo formaldehyde cross-linking confirmed Sp1 factor binding to its *cis*-acting element during the $G_0/G_1$ phase. The functional significance of these Sp1 and X-*Not*I sites was evaluated by transient transfection analysis. Northern blot analysis and nuclear run-off assays revealed maximum DOR mRNA level and transcription rate, respectively, during the $G_0/G_1$ phase of NG108-15 cells. In summary, the protein-DNA interactions at the Sp1 and X-*Not*I sites are necessary for cell cycle-dependent and cell-type–specific up-regulated DOR gene expression.

Opioid receptors referred to as μ, δ, and κ interact with families of endogenous peptides and exogenous opiates such as morphine. The actions of opioids mediated via δ-opioid receptors (DOR) include spinal analgesia, locomotion, limbic effects (Simonds, 1988), and the DOR-mediated neuromodulation. This includes antipropulsive and antisecretory effects in the intestinal tract (Brown et al., 1998). A recent study of DOR knockout mice has demonstrated a loss of morphine tolerance in these animals (Zhu et al., 1999).

The regulation of DOR gene expression has become a subject of continuous study since the cloning of the DOR in 1992 (Evans et al., 1992; Kieffer et al., 1992). Further investigations have shed light on the tissue and cell-type specific expression of this gene (Gaveriaux et al., 1995; Sedqi et al., 1996; Buzas and Cox, 1997). It has also provided a molecular basis for changes in the level of DOR mRNA transcripts under different conditions. These conditions include membrane depolarization (Buzas et al., 1998), treatment of cells with ethanol (Charness et al., 1993), retinoic acid (Beczkowska et al., 1996), nerve growth factor (Abood and Tao, 1995), and anti-CD3-epsilon (Li et al., 1999). Activation of cannabinoid receptor pathway can also increase the amount of DOR transcripts in cell cultures (Di Toro et al., 1998). On the other hand, the activation of the adenylyl cyclase-protein kinase A pathway resulted in down-regulation of DOR gene expression (Buzas et al., 1997; Gylys et al., 1997). In view of these studies, it is important to elucidate the mechanisms underlying temporal DOR gene transcription.

Previously, our laboratory reported the genetic organization of the DOR gene (Augustin et al., 1995). Multiple transcription initiation sites have been mapped in a TATA-less, GC-rich region, between nucleotides −390 and −140 upstream of the translation start codon (+1). Subsequent analysis has led to the identification of the DOR basal promoter (between nucleotides −262 and −141 bp) using in vivo functional assay and in vitro protein-DNA binding assay (Liu et al., 1999). DNA sequence analysis of this region revealed potential binding sites for several transcription factors, such as Sp1, nuclear factor-κB, upstream stimulatory protein, and activator protein-2. However, in vivo interactions of transcription factors with these putative *cis*-acting elements on DOR promoter regions have not been evaluated fully.

At first, one may question the relevance of examining DOR expression in relation to cell cycle. However, much evidence has recently accumulated to support the expression of opioid peptides and receptors in non-neuronal cycling cell types. For example, opioid receptor-mediated immunomodulation in immune cells has been well documented, showing the influence of opioids and the receptors on cytokine gene expression, which are known as the principal communication signals of the immune system (Gaveriaux et al., 1995; Ruzicka and

This research was supported by National Institute of Health research Grants DA00546, DA11806, DA70554, and the A&F Stark fund of the Minnesota Medical Foundation.

**ABBREVIATIONS:** DOR, δ-opioid receptor; Sp1, simian virus 40 promoter factor 1; N2A, Neuro2A cells; DMEM, Dulbecco's modified Eagle's medium; PBS, phosphate-buffered saline; PCR, polymerase chain reaction; bp, base pair(s); GAPDH, glyceraldehyde 3-phosphate dehydrogenase; SSC, standard saline citrate; SV40, simian virus 40; Ab, antibody; kb, kilobase.

Akil, 1997; Brown et al., 1998). Studies of antitumor activity mediated by endogenous δ-opioid peptides (Murgo, 1985; Scholar et al., 1987; Zagon and McLaughlin, 1990) and the DOR-mediated effect on a growth factor-stimulated neuroblastoma tumor cell proliferation (Law and Bergsbaken, 1995) also suggest the possible multifunctional properties of DOR. Furthermore, cell cycle-dependent modulation of DOR gene expression and changes in receptor properties have been demonstrated in previous studies (Scheideler et al., 1983; Sarne and Gafni, 1996). These observations on opioid receptors have led us to examine DOR expression in a defined experimental system.

Our preliminary studies on in vivo footprinting using asynchronous cells expressing endogenous DOR failed to show an apparent protection from dimethyl sulfate methylation at G or A residues in the DOR promoter region. One possible explanation was that a temporary binding of *trans*-acting protein to the 5′ region of the DOR gene might be occurring during the cell cycle, thereby masking the footprinting results when an asynchronous cell population was used. Therefore, in the present study, we tested the hypothesis of the possibility of DOR gene expression in a temporal and restricted manner. In vivo approaches were employed to analyze DOR gene regulation that is transcriptionally controlled by specific transcription factors and the *cis*-acting elements in the basal promoter region. We showed that these DNA-protein interactions were cell-cycle dependent and cell-type specific.

## Experimental Procedures

**Cell Culture and Synchronization.** Mouse neuroblastoma × rat glioma NG108-15 hybrid cells, mouse neuroblastoma NS20Y, and N2A cell lines were maintained under 10% $CO_2$ at 37°C in Dulbecco's modified Eagle's medium (DMEM) with 4.5 g/l D-glucose, L-glutamine, pyridoxine hydrochloride, 110 mg/l sodium pyruvate, 3.65 g/l sodium bicarbonate, 10% heat-inactivated fetal bovine serum, 100,000 U/l penicillin, and 100 mg/l streptomycin sulfate. HAT supplement (1×) was added to the media for cultivation of NG108-15 cells (all ingredients for complete media were from Invitrogen (Carlsbad, CA). Mouse H2.35 hepatoma cells were grown in DMEM with 1.0 g/l D-glucose, 200 nM dexamethasone, and 4% heat-inactivated fetal bovine serum under 10% $CO_2$ at 37°C. NG108-15 and N2A cells were detached by shaking from the growing surface using 1× PBS, and 1× PBS with 1.3 mM EDTA, respectively. For the synchronization procedure, both cell lines were plated at 40 to 50% confluence. Cells were collected in the $G_0/G_1$ phase after 48 h of serum starvation (Scheideler et al., 1983; Sarne and Gafni, 1996). Alternatively, cells were synchronized in the $G_0/G_1$ phase using serum withdrawal for 24 h and also after isoleucine starvation for an additional 24 h. For the isoleucine starvation, we used Dulbecco's modified Eagle's medium without L-isoleucine (Atlanta Biological, Norcross, GA) and the fetal bovine serum extensively dialyzed against Eagle's buffer solution according to the protocol listed (Scheideler et al., 1983). To accumulate cells at the $G_1$/S boundary, the $G_0/G_1$ cultures were incubated in a complete medium with 5 μg/ml aphidicolin (Sigma, St. Louis, MO) for 24 h (Pedrali-Noy et al., 1980). Aphidicolin was removed by washing the cells with the complete medium, followed by incubation in the complete medium for 3 h to allow the cells to enter the S phase. After an additional 7 h, the cells commenced their entry into mitosis. To enrich the population of mitotic cells, gentle washing with 1× PBS collected only nonadherent cells. To obtain cells in the early $G_1$ phase, mitotic cells were replated and incubated in the complete medium for 6 h. A schematic representation of this protocol is shown in Fig. 3A.

**Flow-Cytometric Analysis.** The distribution of cells in different cell cycle phases was monitored by flow cytometry. Approximately $10^6$ cells were harvested and stained with propidium iodide as described previously (Vindelov and Christensen, 1994). Samples were scanned with a FACScalibur cytometer (BD Biosciences, San Jose, CA). Extended analysis of DNA content was performed using ModFit LT software (ver. 2.0; Verity Software House Inc., Topsham, ME).

**In Vivo Genomic Footprinting.** For each genomic footprinting experiment, $10^7$ cells were treated with 0.1% dimethyl sulfate (Aldrich, Milwaukee, WI) for 10 min at room temperature. Each reaction was terminated by the addition of equal volumes of 1 M β-mercaptoethanol and a complete medium. The cells were subsequently harvested and washed once with a complete medium containing β-mercaptoethanol, then twice with 1× PBS. DNA was isolated using the Genomic-tip system (QIAGEN, Valencia, CA) according to the manufacturer's protocol. Piperidine cleavage at methylated and sequencing reactions for genomic DNA were performed according to a standard protocol (Saluz and Jost, 1987). Sequenced and footprinted DNAs were analyzed by ligation-mediated PCR the procedure reported by Quivy and Becker (1993). Five sets of oligonucleotide primers were then used for each footprinting analysis of the 5′

TABLE 1
Sequence of the oligonucleotides used for in vivo DMS footprinting and PCR analysis

| Primer | Genomic Position | Sequence (5′ → 3′) | Annealing Temperature |
|---|---|---|---|
| | | | °C |
| d1F-1 | −441 to −418 | AACTTGAGAGTGCTTAAGCGGCTC | 60 |
| d1F-2 | −432 to −406 | GTGCTTAAGCGGCTCGCTCAAGGTTAC | 68 |
| d1F-3 | −421 to −392 | GCTCGCTCAAGGTTACTCCCATCGTCCGTG | 72 |
| d2F-1 | −303 to −285 | ACCTGGAGTCAGCGGAGCC | 60 |
| d2F-2 | −297 to −277 | AGTCAGCGGAGCCCAGGCAGG | 67 |
| d2F-3 | −283 to −262 | AGGCAGGGAGCGCGCGCGAGGC | 71 |
| d3F-3 | −233 to −213 | TGCAGCGCCCGCCCCCGATCG | 70 |
| d1R-1 | +69 to +48 | AAAGGCGTCCGAGAGGTTGACG | 60 |
| d1R-2 | +58 to +36 | AGAGGTTGACGAGGGGCGAGGAC | 67 |
| d1R-3 | +48 to +25 | GAGGGGCGAGGACTGCAGCTCCGC | 71 |
| d2R-1 | −52 to −71 | AGTGGCGCGCGGAAAACGGA | 60 |
| d2R-2 | −58 to −78 | GCGCGGAAAACGGAGGCCACG | 67 |
| d2R-3 | −68 to −88 | CGGAGGCCACGGCCCCGACGC | 71 |
| d3R-1 | (−128/−111) | CCTCCTCCGCCCGGTCGA | 62 |
| d3R-2 | (−142/−123) | GGTCGACCGCCCGCAGTGCT | 67 |
| d3R-3 | (−150/−128) | ACCGCCCGCAGTGCTCGCCCAAG | 70 |
| G-1 | | ATCACTGCCACCCAGAAGACTGTGGA | 64 |
| G-2 | | GAGCTTGACAAAGTTGTCATTGAGAGC | 64 |
| 28S-1 | | GGACCCGAAAGATGGTGAACTATG | 64 |
| 28S-2 | | ACTCCTTAGCGGATTCCGACTTC | 64 |

region of the DOR gene: sets d1R, d2R, and d3R for the upper strand and sets d1F and d2F for the lower strand (Table 1). Finally, the autoradiograms were scanned with a laser densitometer (Bio-Rad, Hercules, CA) and quantified with the use of the ImageQuant program (Molecular Dynamics, Sunnyvale, CA).

**Metabolic Labeling of Tissue Culture Cells.** For metabolic labeling with [$^{35}$S]cysteine/methionine, radioactivity >1000 Ci/mmol (PerkinElmer Life Science Products, Boston, MA), cells were incubated in cysteine/methionine-free medium (DMEM) for 0.5 h. A [$^{35}$S]cysteine/methionine mix (100 $\mu$Ci/100-mm dish) was then added in 10 ml of cysteine/methionine-free medium containing 10% dialyzed fetal bovine serum (3.5 kDa cut off). The cells were then incubated at 37°C overnight.

**In Vivo Cross-Linking Analysis.** A modified protocol (Dedon et al., 1991) employing a fraction of chromatin with specific antibodies to DNA-binding proteins was used to study protein-DNA interactions. Approximately $10^7$ cells per 100-mm dish were fixed with 1% formaldehyde by direct addition to cultures. After 3 min, the cross-linking reaction was stopped using 0.125 M of glycine. Fixed cells were washed three times at 4°C in ice-cold PBS. The cells were scraped in 2 ml radioimmunoprecipitation assay buffer (150 mM NaCl, 1% Nonidet P-40, 0.5% deoxycholic acid, 0.1% SDS, 50 mM Tris-HCl, pH 7.4) containing a COMPLETE protease inhibitor cocktail (Roche Molecular Biochemicals, Indianapolis, IN) as a source of protease inhibitors. The chromatin was shred to an average DNA fragment size of 500 bp by sonication at 4°C (size of DNA fragments was detected by agarose gel electrophoresis). The sonicated samples were centrifuged (20,000*g*, 5 min) to precipitate insoluble material. The immunoprecipitation reaction using a 1/1000 dilution of rabbit polyclonal Sp1 antibody (Santa Cruz Biotechnology, Santa Cruz, CA) was carried out according to the manufacturer's protocol. After proteinase treatment at 56°C for 1 h, heating at 65°C for 6 h reversed the cross-links and then the DNA was purified by standard methods. Immunoprecipitated DNA was analyzed by PCR. Approximately 1 ng of DNA was used as a template in a 50-$\mu$l PCR reaction mixture using 2.5 U of *Taq*I polymerase, 250 $\mu$M concentrations of each deoxynucleotide (dATP, dCTP, dGTP, and dTTP), and a reaction buffer containing $MgCl_2$ (Roche Molecular Biochemicals). For DOR amplification, primers d2R-3 and d3R-3 (Table 1) were used; a set of primers specific to the GAPDH exon 8 was used for GAPDH amplification (Table 1). The amplification was performed using one cycle at 95°C for 2 min; 35 cycles at 95°C for 40 s; 68°C (for DOR) or 64°C (for GAPDH) for 30 s, and 72°C for 30 s.

**RNA Isolation and Northern Blot Analysis.** Asynchronous cells and cells synchronized at different phases of the cell cycle were collected and the total RNA was isolated using the RNAqueous phenol-free total RNA isolation kit (Ambion, Austin, TX). RNAs (10 $\mu$g per lane) were separated on a 1% agarose/2.2 M formaldehyde gel. The amount of 28S and 18S RNA per lane was quantified after ethidium bromide staining using the Gel Doc 1000 (Bio-Rad) densitometer and analyzed with Molecular Analyst software (Bio-Rad). The RNA was then transferred to a nylon membrane (Hybond-N+) according to the manufacturer's instructions (Amersham Pharmacia Biotech, Arlington Heights, IL). UV cross-linking was carried out for fixation of the RNA to the membrane. RNA blots were prehybridized at 58°C for 1 h in a hybridization solution (5× Denhardt's solution, 5× SSC, 10 mM sodium phosphate buffer, 1 mM EDTA, 0.5% SDS, 100 $\mu$g/ml sonicated and denatured salmon sperm DNA, and 50% formamide). To prepare $^{35}$S-UTP-labeled antisense riboprobes, the following were used as templates: a linearized pcDNA3 (Invitrogen) plasmid containing the mouse DOR cDNA; linearized pBluescript II KS$^+$ plasmid (Stratagene, La Jolla, CA) containing a 200-bp PCR fragment from DOR 5′ untranslated regions, 450 bp of *Sac*I, or 489 bp of *Kpn*I fragments from 3′ untranslated regions; linearized pGEM-2 plasmid (Promega, Madison, WI) with fragment of the mouse $\beta$-actin cDNA. In vitro transcription was performed according to Stratagene instructions for the RNA Transcription kit using Sp6 or T7 RNA polymerases. Northern blots were hybridized with the DOR riboprobe at 58°C overnight. Blots were then washed with 2× SSC/0.1% SDS (three times for 15 min at 50°C) and 0.1× SSC/0.1% SDS (two times for 15 min at 58°C). mRNA levels were visualized with the use of PhosphorImager (Molecular Dynamics). The signal intensity of each hybridization band from two separate Northern blots was calculated using ImageQuant software (Molecular Dynamics). The integrity and amount of RNA on the membrane was further examined by stripping the membrane in 0.1% SDS at 95°C for 10 min and rehybridizing with $\beta$-actin riboprobe as described above.

**Nuclear Run-off Assay.** Nuclei from synchronized NG108-15 cells in the $G_0/G_1$, $G_1$/S, and S phases were used to generate [$^{32}$P]UTP-labeled run-off transcripts. Nuclear RNA was prepared as described previously (Greenberg and Bender, 1993). The labeled RNA was hybridized using slot blots carrying 5-$\mu$g quantities of mouse DOR full-length cDNA (1.8 kb), 1 $\mu$g of a 392-bp fragment of mouse GAPDH coding sequence (exon 8), and 1.3 $\mu$g of a 480-bp fragment of the mouse 28S rRNA coding sequence. GAPDH and 28S probes were synthesized by PCR using primers G1/G-2 and 28S-1/28S-2, respectively (see Table 1).

**Constructs for Luciferase Reporter Assay.** The 5′- and 3′-deletion constructs containing different upstream regulatory sequences of the mouse DOR gene were generated by Dr. L. Augustin (Augustin et al., 1995). For this purpose, the 1.3-kb *Sac*I-*Nco*I fragment containing the DOR gene upstream sequence (position from −1300 to +1 related to the translation start site as +1) was digested with the appropriate restriction enzymes and cloned into the polylinker site of a promoterless and enhancerless luciferase vector, pGL3-basic (Promega). For example, the 5′-deletion construct pD262 contains the DOR gene sequence from −262 to +1 and construct pD1300 contains the DOR gene sequence from −1300 to +1.

Mutant constructs pDm226 and pDm196 were made by Liu et al. (1999) using oligonucleotide-directed PCR mutagenesis. *Hin*dIII linker mutations were introduced into the pD262 original construct. Thus pDm226 represents the mutation construct containing the mutated sequence (AAGCTT) at position −226 to −221; all other pDm constructs contain the mutated sequence in the six nucleotides beginning with the indicated number. Double-mutation construct, pDmD was created by mutation of pDm226 by replacing the sequence at position −196 to −191 with *Xba*I restriction enzyme site. Plasmids for the transient transfection assay were purified by QIAGEN anion exchange columns.

**Transfection and Reporter Gene Assay.** Cells were split and subcultured into a 35-mm, 6-well plate at a density of $0.2 \times 10^6$ cells per well 1 day before transfection. Transient transfections were performed using the SuperFect Transfection reagent (QIAGEN) as described by the manufacturer. To control for differences in transfection efficiency, 0.5 $\mu$g/well of pCH110 DNA (Amersham Pharmacia Biotech, Piscataway, NJ) containing the $\beta$-galactosidase gene was used as an internal control. After 24 h, the cells were washed with ice-cold 1× PBS, harvested, and lysed with an appropriate buffer (Promega, Madison, WI). The luciferase and $\beta$-galactosidase activities of each lysate were determined by a luminometer as indicated by the manufacturers [Promega and Tropix (Bedford, MA), respectively].

## Results

**Localization of DOR Basal Promoter in NG108-15 and Cell-Type Specificity** Recently, we have defined the basal promoter of the DOR gene by conducting 5′- and 3′-serial deletion analysis (Liu et al., 1999). Liu et al. have demonstrated that the promoter sequence between −262 and −141 (position +1 corresponds to the position of the first nucleotide at the ATG translational start codon) is sufficient to provide the DOR basal promoter activity in NS20Y cells, a DOR-expressing neuronal cell line. Subsequent transfection of the 5′- and 3′- deletion constructs into mouse neuroblas-

toma × rat glioma hybrid cell line, NG108-15 have revealed that the sequence from −262 to −141 is sufficient for the DOR basal promoter activity.

To verify the cell-type specific activity of the DOR basal promoter, we performed reporter gene activity assay using different cell lines. NS20Y, NG108-15, N2A, and H2.35 cell lines were transiently transfected with 5′-serial deletion constructs referred to as pD1300, pD890, pD675, pD262, pD182, and pD150 (Fig. 1). These sequences were cloned into the polylinker site of a promoterless and enhancerless luciferase vector pGL3-basic. The pGL3-basic plasmid (designated *Basic*) was included as a negative control, whereas the pGL3-control plasmid (designated *Control*), containing the SV40 promoter and SV40 enhancer was used as a positive control.

As shown in Fig. 1, the luciferase reporter construct pD262 showed 65% relative luciferase activity in DOR-expressing cell lines NS20Y and NG108-15. (The luciferase activity of the positive control plasmid, pGL3-control, was taken as 100%). pD1300, pD890, and pD675 constructs exhibited 52 to 72% activity in these cell lines. Levels of luciferase activity for constructs pD182 and pD150 were near levels of *Basic*. However, no difference was observed among all the constructs when transient transfection was performed using N2A and H2.35 cell lines (Fig. 1). These neuroblastoma N2A and hepatoma H2.35 cells do not express endogenous DOR. Therefore, these data suggested that the DOR basal promoter region from −262 to −182 bp might contain *cis*-acting elements responsible for a cell- or/and tissue-type specific expression of DOR.

**Origin of Multiple DOR Transcripts.** Our previous study has shown that there are multiple transcripts of DOR gene (Evans et al., 1992; Charness et al., 1993). Northern blot analysis also confirmed the previous observation (Fig. 2B). This experiment was conducted by using probes from 5′- and 3′-untranslated regions. Five transcripts of various sizes (2.0, 2.5, 4.5, 6.5, and 8.5 kb) were detected when the cDNA (Fig. 2A, probe 2) was hybridized to mRNA extracted from the DOR-expressing cells lines, NS20Y and NG108-15. When either probe 1, located upstream (position from −440 to −230) from the ATG codon, or probe 4, located 7.5 kb downstream from the TGA stop codon, was used, no transcript specific to the DOR was detected. On the other hand, the probe 3 that is 4.5 kb downstream from TGA hybridized with the two larger transcripts, 6.5 and 8.5 kb (Fig. 2B). The hybridization results using NS20Y and NG108-15 were identical. In contrast, when N2A cells that do not express the endogenous opioid receptor were tested, no hybridizing band was observed. Hybridization to the β-actin probe, which was used as a control, demonstrated the high fidelity of the RNA samples and relative amounts of mRNA (Fig. 2B). These results suggest that the DOR multiple transcripts were different by the size of 3′- untranslated regions.

**In Vivo Footprinting Analysis of Protein-DNA Interactions in the DOR Promoter Using Synchronized Cells.** After determination of the single DOR basal promoter, we investigated protein-DNA interactions in this region using an in vitro assay system. Our preliminary data from in vivo footprinting using an asynchronized cell population showed that there is no protection in the DOR basal promoter region (data not shown) even though our previous study had demonstrated the binding of protein(s) to this region by in vitro method, electrophoretic mobility shift assay. Therefore, we speculated that a temporary binding of a *trans*-acting protein(s) to the corresponding responsible element(s) may have been masked the footprinting results when asynchronous cells were used. To examine whether transcription factors interact with their *cis*-acting elements in the DOR basal promoter, which in turn activates transcription during a specific phase of the cell cycle, we performed the following experiments using synchronized cell populations. NG108-15 is known to express 200,000 DOR molecules per cell (Klee and Nirenberg, 1974), whereas the N2A cell line does not express DOR and was used as a negative control. Both cell lines, NG108-15 and N2A, displayed similar behavior during cultivation and exhibited similar cell cycle characteristics. This enabled us to use the same synchronization protocol for both cell lines (Fig. 3A). Cells enriched in different phases of the cell cycle (e.g., $G_0/G_1$, $G_1$/S border, S, M, and early $G_1$ phases) were obtained (Fig. 3B). It was noted that a serum starvation for more than 2 days led to visible apoptotic changes, suggesting that these cells were not stably synchronized into the $G_0/G_1$ phase.

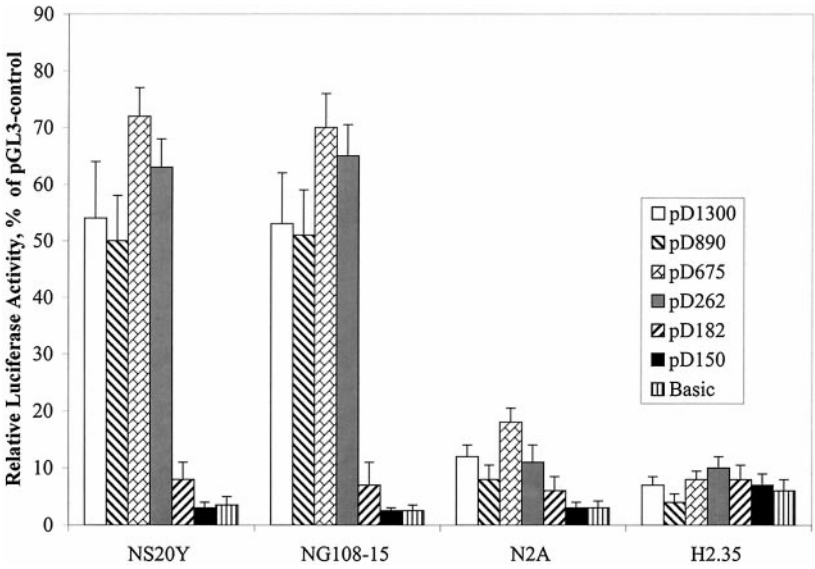


**Fig. 1.** Cell specific activity of the DOR basal promoter. Transient transfection analysis was carried out with neuronal cells NS20Y, NG108-15, N2A, and non-neuronal cells H2.35. Luciferase activities of a series of 5′ deletion constructs were expressed as percentage activity of the pGL3-control plasmid (positive control) containing the SV40 promoter and SV40 enhancer. The pD1300 ~ pD150 constructs contain the DOR promoter region upstream sequence from −1300 ~ −150 to +1, which were fused to luciferase reporter gene system. Nucleotide +1 corresponds to the translation start site (ATG). Note pD262 plasmid contains the minimal functional domain of the DOR promoter. Only endogenous DOR-expressing cell lines, NS20Y, and NG108-15 showed luciferase activity driven by DOR promoter constructs. After transfection, cells were harvested 24 h and a luciferase reporter assay was performed. *Basic* indicates for the pGL3-basic plasmid used as a negative control. Transfection efficiencies were normalized to the β-galactosidase activity by co-transfecting the pCH110 plasmid as an internal control. The data shown are means ±S.E. of three independent transfection experiments with at least two different plasmid preparations.

We used two approaches for the synchronization of these cells as described under *Experimental Procedures*. Cells harvested in different phases of the cell cycle were used in an in vivo footprinting assay with primer sets covering the basal promoter region. Five different primer sets were used for this analysis. The location of each primer is indicated in Fig. 4A and Table 1.

Each primer set contains three overlapping oligonucleotides: sets d1F and d2F correspond to sequences of the upper strand in the promoter region of the DOR gene, whereas sets d1R, d2R, and d3R correspond to sequences of the lower strand. These primers allowed analysis of the 400-bp region (from −385 to +23, where +1 corresponds to the position of the first nucleotide in the ATG translational start codon). When d2F primers were used (from −259 to −172), two footprints were detected on the lower strand of the DOR gene 5′- region in the $G_0/G_1$ phase of the NG108-15 cells. However, there was no footprint when N2A cells were used (Fig. 4B). The first footprint corresponded to the Sp1 binding site, and the second footprint overlapped a site for *Not*I restriction endonuclease, referred to as X-*Not*I. Densitometric analysis of the autoradiograms quantitatively confirmed this protection. Interestingly, protection was only slightly visible during early $G_1$ phase (6 h after mitosis). The d3R primers demonstrated the complete protection of the Sp1 and partial protection of X-*Not*I sites for NG108-15 cells on the upper strand in the $G_0/G_1$ phase. No protection was observed when primers, d1F, d2R, and d1R were used.

**Analysis of Sp1-DNA Interaction by in Vivo Formaldehyde Cross-Linking.** The Sp1 binding to the responsible element on the DOR basal promoter was confirmed in vivo with the use of a formaldehyde cross-linking approach. Cells synchronized in different phases of the cell cycle were fixed by 1% formaldehyde followed by immunoprecipitation of the Sp1-DNA complexes after chromatin solubilization. To perform high-resolution mapping of binding sites using this approach, it was important that the final DNA fragments be smaller than 500 bp. After chromatin solubilization, Sp1-DNA complexes were immunoprecipitated with rabbit polyclonal Ab against Sp1. In our preliminary experiments, specific immunoprecipitation was demonstrated during 1-h incubation at 4°C with a 1/1000 dilution of antibodies (Fig. 5A). Cross-linking was reversed by heat treatment followed by PCR amplification of the immunoprecipitated DNA. PCR amplification was performed with d2F-3 and d3R-3 primers that were specific for the DOR promoter region. We used several negative controls in this procedure to detect levels of background: absence of Anti-Sp1 Ab during immunoprecipitation; normal rabbit serum instead of Anti-Sp1 Ab, and a non–cross-linked sample. To estimate a level of possible background we also performed a PCR analysis with primers specific to exon 8 of the GAPDH gene. Several dilutions of genomic DNA (10 ng, 5 ng, and 2.5 ng) were used as additional control for PCR. The ratio of DOR and GAPDH PCR fragments in samples with genomic template was around 1:2 because of a different efficacy of PCR with a different set of primers.

In the case of NG108-15–immunoprecipitated samples, we observed a uniform level of background using GAPDH primers (Fig. 5B). The amount of PCR fragment corresponding to the DOR promoter was significantly higher than the background in the case of NG108-15 cells in $G_0/G_1$ and $G_1$ phases

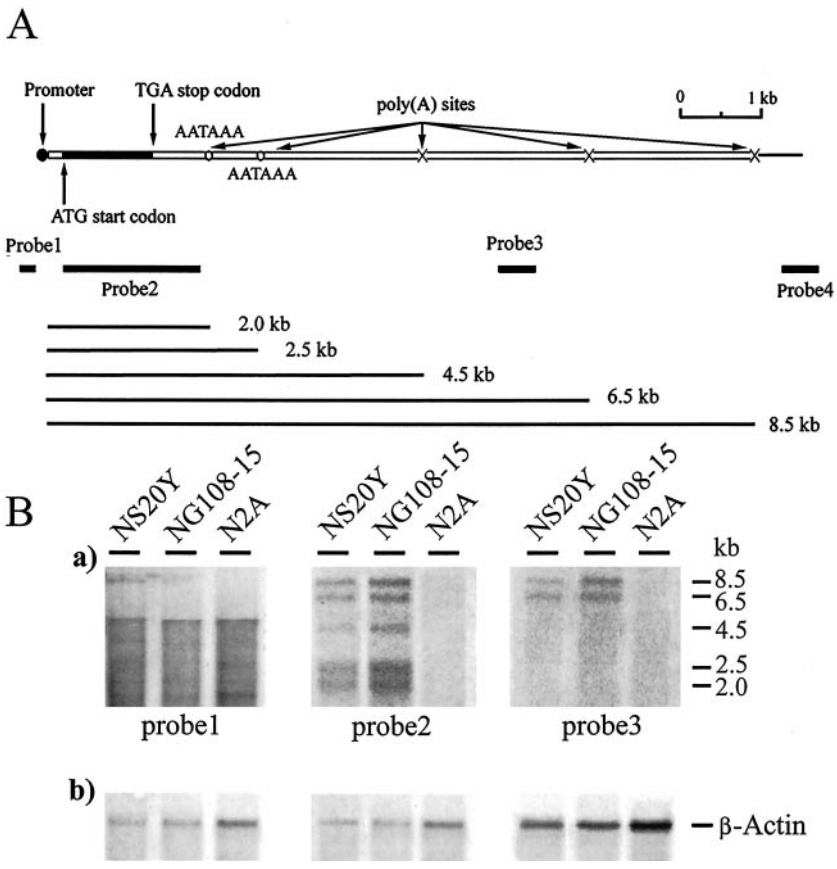


**Fig. 2.** Mapping of the multiple DOR gene transcripts. A, structure of the mouse DOR cDNA. The closed bar represents the coding region from the ATG translation start codon to the TGA translation stop codon; open bar indicates the 3′-untranslated region; ○ and × represent poly(A) and putative poly(A) sites, respectively. Four probes were used for Northern blot analysis: probe 1, 200-bp PCR fragment upstream of the basal promoter; probe 2, 1.8-kb DOR cDNA; probe 3, 450-bp *Sac*I fragment subcloned from genomic DNA library; probe 4, 489-bp *Kpn*I fragment subcloned from genomic DNA library. Bottom five lines indicate five DOR transcripts. B, a, Northern blot analyses. DOR mRNA extracted from NG108-15, NS20Y, and N2A cells were hybridized with the four probes. The sizes of the bands were estimated from mRNA marker. Probe 2 hybridized to the five DOR transcripts only in NG108-15 and NS20Y cells. Probe 3 detected two larger transcripts. No DOR transcript was detected from N2A cells. Probes 1 and 4 (data not presented) showed no hybridization for all cell lines tested. Each sample contains 1 $\mu$g of poly(A) RNA. b, hybridization with $\beta$-actin probe shows high level of fidelity of the RNA samples.

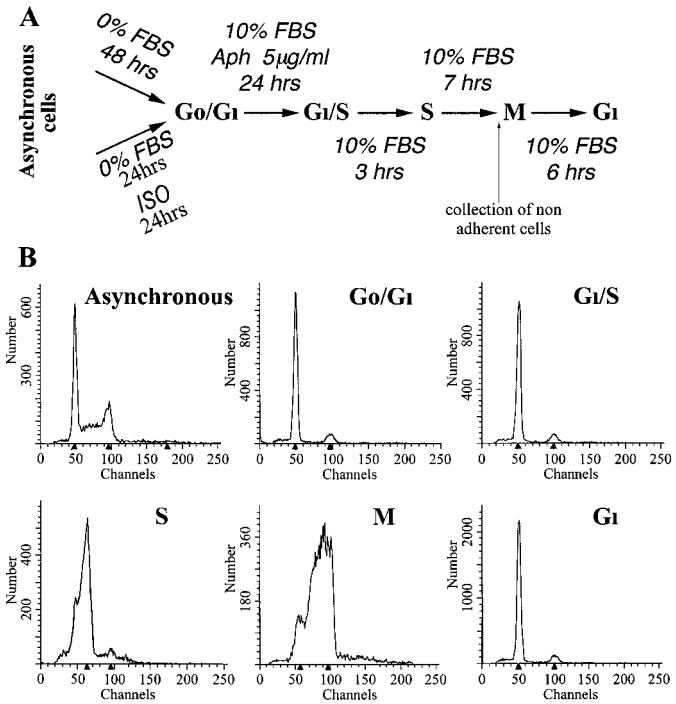


**Fig. 3.** Synchronization of NG108-15 hybrid cells. A, schematic representation of the synchronization protocol. B, flow cytometric analysis of propidium iodide-stained asynchronous cells and cells synchronized in various phases of the cell cycle. At least $10^5$ cells were analyzed per sample.

(Fig. 5B). Densitometer analysis showed that the DOR: GAPDH PCR fragments ratio was 10:1 and 5:1, respectively. The ratios for these samples were 20 and 10 times higher compared with samples with control genomic DNA, respectively. These results demonstrated that transcription factor Sp1 bound to its binding site in the DOR basal promoter region in NG108-15 cells during the $G_0/G_1$ phase of the cell cycle.

**Functional Analysis of the *cis*-Elements Present in the DOR Basal Promoter.** To verify the functional significance of the Sp1 and X-NotI sites in the DOR promoter region, PCR mutants of pD262 construct were used (see *Experimental Procedures*). This original construct contains the 0.26-kb DNA fragment of DOR basal promoter. The *Basic* plasmid containing no promoter was included as a negative control, whereas the *Control* containing the SV40 promoter and enhancer was used as a positive control. The mutant constructs and control plasmids were transiently transfected into NG108-15 cells and the promoter activities were assayed by measuring luciferase activity.

As shown in Fig. 6, NG108-15 cells transiently transfected with Sp1 or X-*Not*I mutant constructs demonstrated decreased luciferase activities up to 70% and 60%, respectively. Double mutation of these sites showed the synergistic effect and led to a decrease of up to 90%, almost abolishing the basal DOR promoter activity. These results demonstrated that both Sp1 and X-*Not*I binding sites were critical for basal DOR gene expression.

**Northern Blot Analysis of DOR mRNA during Cell Cycle.** To verify a correlation between the DNA-protein interactions shown by the footprinting analysis and the transcribed DOR mRNA levels, aliquots of total RNA from synchronized NG108-15 cells, as well as from asynchronous NG108-15 and N2A cells were subjected to Northern blot analysis. Hybridization of the DOR riboprobe (equivalent to

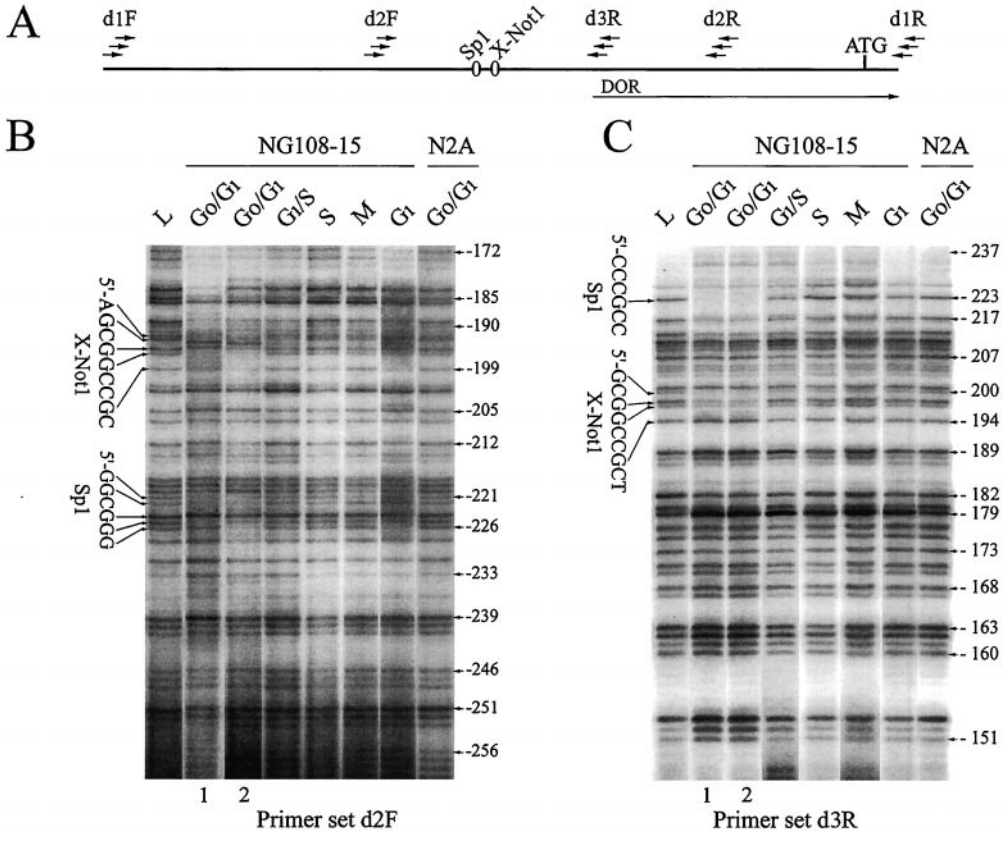


**Fig. 4.** In vivo genomic footprinting of the mouse DOR gene promoter from NG108-15 and N2A cells, synchronized in various phases of the cell cycle. A, positions of primer sets for genomic footprinting. The primer sets d1F, d2F were for screening of the lower strand; d1R, d2R, and d3R were used for upper strand. No footprint was detected with the primers d1F, d1R, and d2R. Primer set d2F visualized sequences from nucleotides −258 to −172. Primer set d3R represented sequences from nucleotides −151 to −237. B, genomic footprint for the lower strand of the DOR basal promoter region (position −258/−172). Note footprints corresponding to Sp1 and X-*Not*I binding sites in the $G_0/G_1$ phase in NG108-15 cells, but not in N2A. The G+A sequencing reaction products are shown in lane L (ladder). Lines 1 and 2 for $G_0/G_1$ correspond to cells synchronized by isoleucine and serum starvation, respectively. Both approaches demonstrated similar results. C, genomic footprint for the upper strand of the DOR basal promoter region (position −151/−237). All lanes/conditions are as in B. Note footprints corresponding to Sp1 and X-*Not*I binding sites in the $G_0/G_1$ phase in NG108-15 cells.

probe 2 in Fig. 2A) with total RNA from NG108-15 cells generated five main bands of 8.5, 6.5, 4.5, 2.5, and 2.0 kb. These results were consistent with our previous Northern blot analysis in this study (Fig. 2B: probe 2). However, a 4.5-kb mRNA transcript was not obvious, possibly because of the presence of significant amounts of 28S rRNA in the total RNA samples that may have comigrated at the same position causing masked hybridization results. It should be noted that no DOR transcripts were detected when N2A cells were used. Although hybridization with the β-actin probe illustrated the high fidelity of RNA used (Fig. 7A, b), the levels of β-actin mRNA varied during the cell cycle [Fig. 7B, b, and (Pardee, 1989)]. Therefore, the β-actin mRNA was not used for subsequent quantitative normalization; rather, 28S and 18S rRNA were used as an internal control to correct for unequal loading in further experiments (Fig. 7A, c, and the histogram in Fig. 7B, c). Quantification of DOR mRNA by PhosphorImager is depicted in Fig. 7B, a. The highest levels of multiple DOR transcripts corresponded to the $G_0/G_1$ phase of the cell cycle. The steady state levels of four representative mRNA species were decreased at the $G_1$/S boundary. There are, however, some transient increases in the amount of the largest transcript (e.g., 8.5 kb), that were observed after release from the aphidicolin block in the S phase. Minimal levels of DOR mRNA were detected in the M and early $G_1$ phases. Interestingly, the amount of larger transcripts (8.5 and 6.5 kb) was increased to a significantly greater extent than those of the smaller transcripts. The mRNA levels of the 8.5- and 6.5-kb transcripts in the $G_0/G_1$ phase were increased up to 7 and 6.5 times, respectively, whereas the levels of the smaller mRNA species, 2.5 and 2.0 kb, were increased to a maximum of 3 times in $G_0/G_1$ phase compared with the levels of transcripts in the M or early $G_1$ phase (Fig. 7B, a). Taken together, these results strongly demonstrated a corresponding relationship between the protein bindings to the binding sites of the basal promoter region and the up-regulated DOR mRNA level in the $G_0/G_1$ phase.

**Analysis of DOR Transcriptional Rate by Nuclear Run-off Assay.** Northern blot analysis is a reflection of steady state level of mRNA. Therefore, to verify that these increases in DOR mRNA during the cell cycle reflect up-regulation of the transcription rather than a reduced mRNA degradation rate, a nuclear run-off assay was performed. Nuclei from synchronized NG108-15 cells were prepared followed by [$^{32}$P]UTP labeling. We were unable to isolate enough amounts of nuclear RNA from the cells in M phase because of the low transcriptional activity in this phase. The labeled nuclear RNA was hybridized to slot blots with 5 μg of immobilized mouse DOR cDNA (1.8 kb) and 1 μg of a 392-bp fragment of the mouse GAPDH coding sequence or 1.3 μg of a 480-bp fragment of the mouse 28S rRNA coding sequence. As shown in Fig. 8, active transcription of the DOR gene was observed only in the $G_0/G_1$ phase; whereas, the GAPDH and 28S rRNA genes were transcriptionally active throughout the cell cycle. These results demonstrated that the transcriptional activity was responsible for the increased level of DOR mRNA during $G_0/G_1$ phase.

As we mentioned above, Northern analysis displayed five transcripts throughout all the phases of the cell cycle (Figs. 2 and 7A, a). In our nuclear run-off assay, however, we were able to detect the transcription of the DOR gene only in the $G_0/G_1$, but not in the other phase of cell cycle (Fig. 8). Considering the half-life of the DOR mRNA, which is approximately 6 h (Buzas et al., 1997), this discrepancy may be caused by the limited sensitivity of the nuclear run-off assay, where probably the remaining amount of surviving mRNA was able to be detected by Northern assay.

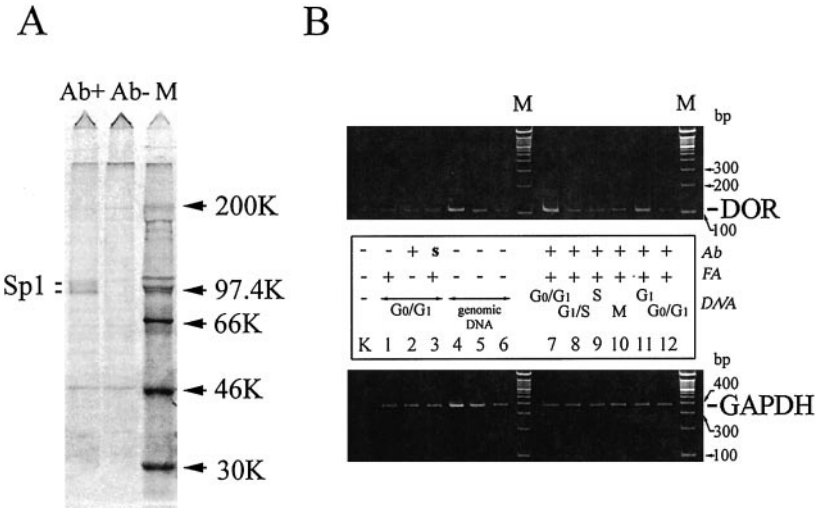


**Fig. 5.** Analysis of Sp1-DNA interaction using formaldehyde cross-linking. A, SDS-polyacrylamide gel electrophoresis of immunoprecipitated proteins. Ab+, immunoprecipitation of Sp1 from [$^{35}$S]cysteine/methionine-labeled NG108-15 cells using rabbit polyclonal anti-Sp1 antibody detected both p95 and p106 Sp1 proteins; Ab−, immunoprecipitation in the presence of rabbit preimmune serum, but in the absence of anti-Sp1 antibody, used as a negative control. M, [$^{14}$C]methylated rainbow marker. B, PCR analysis of the DNA obtained from immunoprecipitation of cross-linked chromatin with anti-Sp1 antibody. Only NG108-15 cells in $G_1/G_0$ or $G_1$ phases showed Sp1 protein-DNA interaction in the DOR promoter region. The middle panel illustrates the varied conditions. Ab, anti-Sp1 antibody; s, preimmune serum was used instead of anti-Sp1 antibody; FA, formaldehyde; DNA, synchronized cells were cross-linked with (+) or without (−) formaldehyde followed by nuclear protein immunoprecipitation with (+) or without (−) Ab. The DNA was purified from the immunoprecipitate. PCR was performed using specific primers from DOR promoter region (d3F-3 and d3R-3). Level of background was detected in all samples after immunoprecipitation using specific primer for exon 8 of the mouse GAPDH gene. Lane M, −100-bp DNA ladder. Lane K, a negative control of PCR. Lanes 1, 2, 3, and 7, $G_0/G_1$ phase NG108-15 cells were cross-linked with (lane 1, 2, 3, and 7) or without (lane 1) Ab or with serum (lane 3). Lanes 4 to 6, a positive control of PCR in the presence of 10, 5, and 2.5 ng of genomic DNA, respectively. Lanes 8 to 11, NG108-15 cells in different phases of cell cycle were cross-linked with formaldehyde and immunoprecipitated with Ab. Lane 12, $G_0/G_1$ phase N2A cells, used as a negative control.

## Discussion

In the present study, we showed that DOR gene transcription was regulated in a cell-cycle–dependent manner. In NG108-15 cells, the highest transcription of DOR occurred in the $G_0/G_1$ phase of the cell cycle, which seemed to be mediated by a transcription factor Sp1. The protein-DNA interaction in the X-*Not*I site in the promoter region also correlated with up-regulation of the DOR gene transcription in $G_0/G_1$.

We also demonstrated that the Sp1 factor binding activity to its *cis*-acting element present in the core DOR promoter was cell-type specific (Figs. 4 and 5). Unlike other opioid receptors, such as the $\mu$-opioid receptor, transiently transfected DOR promoter exhibited cell- and tissue-type specific expression pattern demonstrating preferential expression in endogenous DOR-expressing cell lines, such as NS20Y and NG108-15. The transient transfection with construct containing DOR promoter into non-neuronal cells H2.35 or non-opioid receptor expressing cells N2A showed no significant level of promoter activity (Fig. 1). This cell- and tissue-type specific expression pattern still remained in the shortest promoter construct, pD262, suggesting that the determining element(s) for the cell- and tissue-type specific expression is within the basal promoter region. The mechanisms of the cell-type–specific expression pattern of DOR gene seemed to be correlated with the differential bindings of transcription factors to the *cis*-acting element in the basal promoter region in different cell types. From in vivo footprinting assay, it was noted that in N2A cells that do not express endogenous DOR, no footprint in the basal promoter region was observed, whereas in NG108-15 cells, endogenous DOR-expressing cell line, partial (X-*Not*I) or complete (Sp1) footprints were observed in $G_0/G_1$ (Figs. 4 and 5).

The Sp1 is ubiquitously expressed in murine cells (Saffer et al., 1991), suggesting that most mammalian cells require Sp1 to function properly. It has been found that more than 1000 promoters have GC-rich binding sites for Sp1. Consequently, the Sp1-knockout embryos are severely retarded in development and they die around day 11 of gestation (Marin et al., 1997). The presence of the Sp1 factor in NG108-15, NS20Y, and N2A cells, has been reported. Nevertheless, the cell-cycle–specific Sp1-DNA interaction, which was shown in DOR-expressing cell line, NG108-15, did not occur in N2A from in vivo assays, footprinting (Fig. 4), and cross-linking (Fig. 5). In vivo formaldehyde cross-linking results provided convincing evidence for the cell type-specific Sp1 binding to the DOR basal promoter region, in this case associated with the cell cycle dependence. In agreement with results of the footprinting assay, the interaction between transcription factor, Sp1, and its binding site in the basal DOR promoter was detected during $G_0/G_1$ in NG108-15 cells (Fig. 5). On the other hand, in N2A cells, no cross-linking was observed (Fig. 5B). These results suggest that the expression of DOR gene might be regulated through the cell-type–specific interaction of Sp1 in $G_0/G_1$. We did not find significant difference in Sp1 level during cell cycle for NG108-15 using immunostaining approach (data not shown). Probably, Sp1 binding to DNA is not directly dependent on the protein amount. We suppose that activation of Sp1 binding has complex mechanism. The temporal character of the Sp1 interaction with DOR promoter may depend on the phosphorylation of the C terminus of this factor. The presence and possible interaction with X-*Not*I is also essential. Other transcription factors and co-factors could be involved in Sp1 activation (for review, see Suske, 1999). Involvement or cooperation of another level of

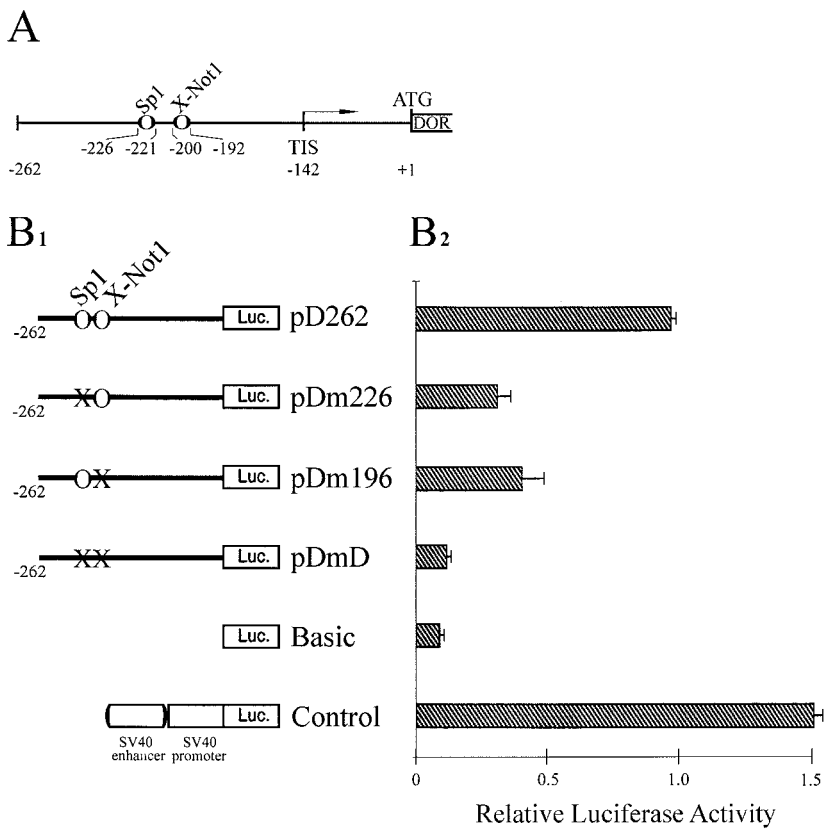


**Fig. 6.** Functional analysis of the Sp1 and X-*Not*I sites in the DOR promoter. A, position of the two putative *cis*-elements Sp1 and X-*Not*I in the DOR basal promoter (pD262). TIS, transcription initiation site; ATG, translation start codon. $B_1$, schematic representation of the recombinant luciferase reporter gene constructs. pD262 contains the original sequence of the mouse DOR basal promoter. pDm226, Sp1 site mutant; pDm196, X-*Not*I site mutant; pDmD, double mutant, mutations in Sp1 and X-*Not*I sites. *Basic* and *Control* indicate the pGL3-basic and pGL3-control vectors used as negative and positive controls, respectively. ×, side(s) that has been mutated. $B_2$, histogram of relative luciferase activity. Luciferase activity for both single or double mutants was reduced significantly. Each mutant construct was transiently transfected into NG108-15 cells. The cells were harvested after 24 h, and assayed for luciferase activity. Transfection efficiency was normalized to the $\beta$-galactosidase activity of pCH110 plasmid that was cotransfected as an internal control. The relative fold activation was measured by luciferase activities. The data shown are means ± S.E. of three independent transfection experiments with at least two different plasmid preparations. *Luc*-luciferase reporter gene.

control mechanism, such as chromatin structure, that can regulate the *cis*/*trans* interactions associated with the cell- or tissue-specific expression of the DOR gene may not be ruled out. Some locus control regions are also considered to provide a dominant cell type-specific open chromatin domain that is easily accessible to transcription factors (Ortiz et al., 1997). Our future studies will be focused on examining these possibilities.

Further investigation by nuclear run-off analysis demonstrated the increased mRNA level that in turn reflected cell-cycle–specific up-regulation of DOR transcription during $G_0/G_1$ (Fig. 8). Northern blot analysis (Fig. 7) also showed an increased abundance of the DOR transcripts in a cell-cycle–specific manner. These data suggest that Sp1 and the unknown factor, which binds to X-*Not*I site, might directly participate in the regulation of cell- and/or tissue-type specific transcription of DOR gene during $G_0/G_1$.

As mentioned in the introduction, the modulatory role of the DOR in cell proliferation and survival is still under investigation. Possibly in the near future some relationship between the DOR gene regulation and these new functions of the receptor will be found.

Functional analysis of these sites by luciferase assay (Fig. 6) also supports the significant role of both *cis*-elements for the expression of the DOR gene. Identification of the unknown *trans*-factor binding to the X-*Not*I site and the investigation of the possible protein-protein interaction between Sp1 and X-*Not*I-binding factors may lead to better understanding of cell- and/or tissue-type specific expression of DOR gene regulation. The Sp1 factor is vital for cell function and absence of this factor leads to a lethal phenotype in mice, as mentioned above (Marin et al., 1997). The creation of a knock-in mouse with a DOR gene, which has a mutated and inactive Sp1 site in the promoter, will be valuable to investigate the role of Sp1 in the receptor gene expression in vivo.

As was reported under *Results* section, multiple transcripts of mouse DOR gene (8.5, 6.5, 4.5, 2.5, and 2.0 kb) were detected in both cell lines, NS20Y and NG108-15 (Figs. 2 and 7). During the process of defining DOR basal promoter region by transient transfection analysis, it was strongly suggested that the DOR gene expression was mediated by a single major promoter, located between −262 and −141 upstream of the ATG codon (+1). Indeed, this is in agreement with the previous analysis on DOR transcripts by reverse transcription-PCR (Gaveriaux-Ruff et al., 1997), in which there is no alternative mDOR cDNA isoform when mRNA from NG108-15 cells is used. A previous report on genomic structure of the DOR gene (Augustin et al., 1995) has determined that polyadenylation begins within a group of four A residues located 1240 to 1243 bp downstream of the TGA stop codon. This position correlates with the size of a 2.5-kb transcript. The shortest 2.0-kb transcript correlates with position of the second polyadenylation signal at 706 bp downstream from the TGA stop codon. Northern blot analysis (Fig. 2, A and B) showed the DOR transcripts different in size of 3′-untranslated regions. Taken together, the previous report and our results, we propose that the DOR multiple transcripts are different by the size of 3′-untranslated regions, possibly because of the alternative polyadenylation signals. However, we do not rule out the possibility that splicing events in the 3′-untranslated regions cause the five different transcripts.

At least two transcripts for rat (4.5 and 11 kb) and human DOR mRNA (7.0 and 11 kb) have also been reported (Fukuda et al., 1993; Beczkowska et al., 1997). The possible functional or regulatory role of mouse, rat, and human DOR multiple transcripts, as well as the relationship of these multiple

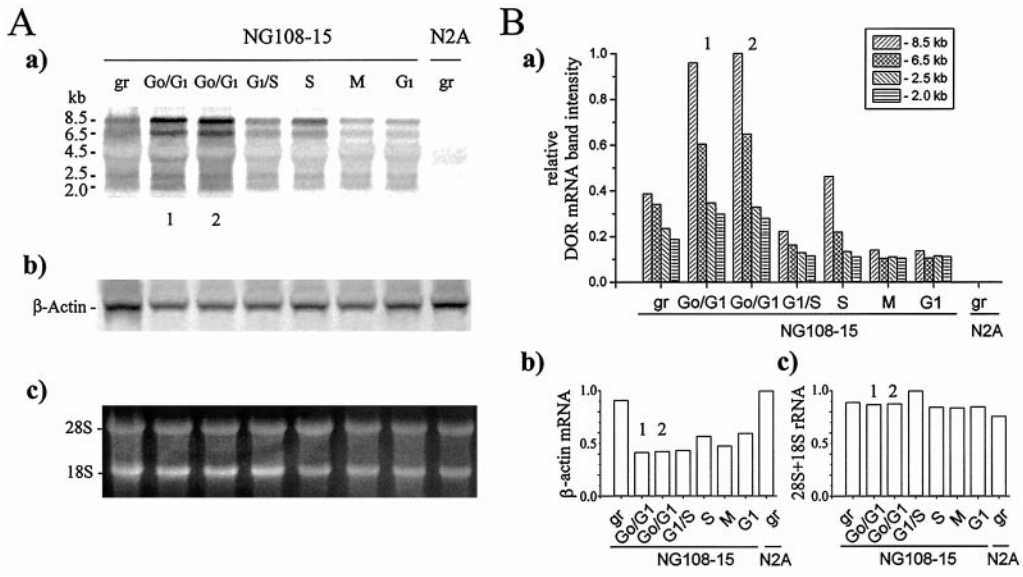


**Fig. 7.** Cell cycle-dependent expression of the mouse DOR gene. A, a, Northern blot analyses of DOR mRNA extracted from asynchronous (gr) or synchronized NG108-15 and N2A cells. The sizes of the bands are estimated from mRNA marker. Note increased intensity of DOR transcripts of all sizes in the $G_0/G_1$ phase and transient increase of 8.5-kb transcript in the S phase in NG108-15 cells. No DOR transcripts detected from N2A cells. b, hybridization with β-actin probe shows high level of fidelity of the RNA samples; c, densitometric picture of 18S and 28S rRNA to correct unequal loading of the RNA samples. B, a, histogram of DOR mRNA level during the cell cycle of NG108-15 and N2A cells. This histogram is normalized to the amount of 18S + 28S rRNA and represented as relative intensity. Note the intensity is maximal in the $G_0/G_1$ phase for all bands, in the S phase there is a transient increase of the 8.5-kb transcript. b, histogram of the relative amount of the β-actin mRNA during the cell cycle; c, histogram of the relative amount of the 18S + 28S rRNA in RNA samples. Numbers 1 and 2 correspond to cells synchronized by isoleucine and serum starvation, respectively. Both synchronization approaches demonstrated the same result.

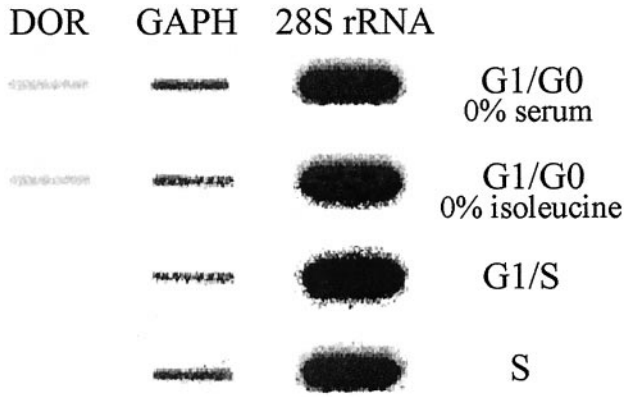


**Fig. 8.** Nuclear run-off transcription assay for DOR gene transcription during cell cycle. Relatively active transcription of the DOR gene is seen only in the G1/$G_0$ phase. The GAPDH and 28S rRNA gene transcription was active in all tested phases of cell cycle. For this study, nuclei from NG108-15 cells synchronized in the $G_0/G_1$ (using serum or isoleucine starvation), $G_1$/S and S phases were used to generate [$^{32}$P]UTP-labeled run-off transcripts. The labeled RNA was hybridized to slot blots carrying 5-$\mu$g quantities of the mouse DOR cDNA (1.8 kb), 1 $\mu$g of a 392-bp fragment of the mouse GAPDH coding sequence, and 1.3 $\mu$g of a 480-bp fragment of the mouse 28S rRNA coding sequence. Numbers 1 and 2 correspond to cells synchronized by isoleucine and serum starvation, respectively. Both synchronization approaches demonstrated similar results.

transcripts to the identified DOR subtypes remains to be determined. Our DNA sequence analysis for the comparison between mouse and human DOR genes revealed up to 95% homology between mouse DOR promoter region (from −255 to −168) and human DOR gene sequences (from −338 to −250). For human, the DOR basal promoter has not been identified. Considering the location of mouse basal promoter (−262 ~ −141 upstream of ATG translation start codon), the homologous region of human DOR gene located between −338 and −250 upstream of the ATG translation start codon (+1) may be a candidate for a human DOR basal promoter. It also suggests that a common mechanism seems to be conserved in the transcriptional regulation of the DOR gene among species.

**Acknowledgments**

We would like to thank Dr. Chih-Hao Lee and Dr. Louisa Nutter for his valuable suggestions.

**References**

Abood ME and Tao Q (1995) Characterization of a delta opioid receptor in rat pheochromocytoma cells. *J Pharmacol Exp Ther* **274:**1566–1573.
Augustin LB, Felsheim RF, Min BH, Fuchs SM, Fuchs JA and Loh HH (1995) Genomic structure of the mouse delta opioid receptor gene. *Biochem Biophys Res Commun* **207:**111–119.
Beczkowska IW, Buck J and Inturrisi CE (1996) Retinoic acid-induced increase in delta-opioid receptor and *N*-methyl-D-aspartate receptor mRNA levels in neuroblastoma x glioma (NG108-15) cells. *Brain Res Bull* **39:**193–199.
Beczkowska IW, Gracy KN, Pickel VM and Inturrisi CE (1997) Inducible expression of *N*-methyl-D-aspartate receptor, and delta and mu opioid receptor messenger RNAs and protein in the NT2-N human cell line. *Neuroscience* **79:**855–862.
Brown DR, Poonyachoti S, Osinski MA, Kowalski TR, Pampusch MS, Elde RP and Murtaugh MP (1998) Delta-opioid receptor mRNA expression and immunohistochemical localization in porcine ileum. *Dig Dis Sci* **43:**1402–1410.
Buzas B and Cox BM (1997) Quantitative analysis of mu and delta opioid receptor gene expression in rat brain and peripheral ganglia using competitive polymerase chain reaction. *Neuroscience* **76:**479–489.
Buzas B, Rosenberger J and Cox BM (1997) Regulation of delta-opioid receptor mRNA levels by receptor-mediated and direct activation of the adenylyl cyclase-protein kinase A pathway. *J Neurochem* **68:**610–615.
Buzas B, Rosenberger J and Cox BM (1998) $Ca^{2+}$/calmodulin-dependent transcriptional activation of delta-opioid receptor gene expression induced by membrane depolarization in NG108-15 cells. *J Neurochem* **70:**105–112.
Charness ME, Hu G, Edwards RH and Querimit LA (1993) Ethanol increases δ-opioid receptor gene expression in neuronal cell lines. *Mol Pharmacol* **44:**1119–1127.
Dedon PC, Soults JA, Allis CD and Gorovsky MA (1991) A simplified formaldehyde fixation and immunoprecipitation technique for studying protein-DNA interactions. *Anal Biochem* **197:**83–90.
Di Toro R, Campana G, Sciarretta V, Murari G and Spampinato S (1998) Regulation of delta opioid receptors by delta9-tetrahydrocannabinol in NG108-15 hybrid cells. *Life Sci* **63:**L197–L204.
Evans CJ, Keith DE Jr, Morrison H, Magendzo K and Edwards RH (1992) Cloning of a delta opioid receptor by functional expression. *Science (Wash DC)* **258:**1952–1955.
Fukuda K, Kato S, Mori K, Nishi M and Takeshima H (1993) Primary structures and expression from cDNAs of rat opioid receptor delta- and mu-subtypes. *FEBS Lett* **327:**311–314.
Gaveriaux C, Peluso J, Simonin F, Laforet J and Kieffer B (1995) Identification of kappa- and delta-opioid receptor transcripts in immune cells. *FEBS Lett* **369:**272–276.
Gaveriaux-Ruff C, Peluso J, Befort K, Simonin F, Zilliox C and Kieffer BL (1997) Detection of opioid receptor mRNA by RT-PCR reveals alternative splicing for the delta- and kappa-opioid receptors. *Brain Res Mol Brain Res* **48:**298–304.
Greenberg ME and Bender TP (1993) Identification of newly transcribed RNA, in *Current Protocols in Molecular Biology* (Ausubel FM, Brent R, Kingston RE, Moore DD, Seidman JG, Smith JA, and Struhl K eds) 4.10.11–14.10.19, Wiley Interscience, New York.
Gylys KH, Tran N, Magendzo K, Zaki P and Evans CJ (1997) cAMP decreases steady-state levels of delta-opioid receptor mRNA in NG108-15 cells. *Neuroreport* **8:**2369–2372.
Kieffer BL, Befort K, Gaveriaux-Ruff C and Hirth CG (1992) The delta-opioid receptor: isolation of a cDNA by expression cloning and pharmacological characterization [published erratum appears in *Proc Natl Acad Sci USA* 1994;91:1193]. *Proc Natl Acad Sci USA* **89:**12048–12052.
Klee WA and Nirenberg M (1974) A neuroblastoma times glioma hybrid cell line with morphine receptors. *Proc Natl Acad Sci USA* **71:**3474–3477.
Law PY and Bergsbaken C (1995) Properties of delta opioid receptor in neuroblastoma NS20Y: receptor activation and neuroblastoma proliferation. *J Pharmacol Exp Ther* **272:**322–332.
Li MD, McAllen K and Sharp BM (1999) Regulation of delta opioid receptor expression by anti-CD3-epsilon, PMA, and ionomycin in murine splenocytes and T cells. *J Leukoc Biol* **65:**707–714.
Liu HC, Shen JT, Augustin LB, Ko JL and Loh HH (1999) Transcriptional regulation of mouse delta-opioid receptor gene. *J Biol Chem* **274:**23617–23626.
Marin M, Karis A, Visser P, Grosveld F and Philipsen S (1997) Transcription factor Sp1 is essential for early embryonic development but dispensable for cell growth and differentiation. *Cell* **89:**619–628.
Murgo AJ (1985) Inhibition of B16-BL6 melanoma growth in mice by methionine-enkephalin. *J Natl Cancer Inst* **75:**341–344.
Ortiz BD, Cado D, Chen V, Diaz PW and Winoto A (1997) Adjacent DNA elements dominantly restrict the ubiquitous activity of a novel chromatin-opening region to specific tissues. *EMBO J* **16:**5037–5045.
Pardee AB (1989) G1 events and regulation of cell proliferation. *Science (Wash DC)* **246:**603–608.
Pedrali-Noy G, Spadari S, Miller-Faures A, Miller AO, Kruppa J and Koch G (1980) Synchronization of HeLa cell cultures by inhibition of DNA polymerase alpha with aphidicolin. *Nucleic Acids Res* **8:**377–387.
Quivy JP and Becker PB (1993) An improved protocol for genomic sequencing and footprinting by ligation-mediated PCR. *Nucleic Acids Res* **21:**2779–2781.
Ruzicka BB and Akil H (1997) The interleukin-1beta-mediated regulation of proenkephalin and opioid receptor messenger RNA in primary astrocyte-enriched cultures. *Neuroscience* **79:**517–524.
Saffer JD, Jackson SP and Annarella MB (1991) Developmental expression of Sp1 in the mouse. *Mol Cell Biol* **11:**2189–2199.
Saluz HP and Jost JP (1987) *A Laboratory Guide to Genomic Sequencing: The Direct Sequencing of Native Uncloned DNA*. Birkhauser, Boston.
Sarne Y and Gafni M (1996) Determinants of the stimulatory opioid effect on intracellular calcium in SK-N-SH and NG108-15 neuroblastoma. *Brain Res* **722:**203–206.
Scheideler MA, Lockney MW and Dawson G (1983) Cell cycle-dependent expression of specific opiate binding with variable coupling to adenylate cyclase in a neurotumor hybrid cell line NG108-15. *J Neurochem* **41:**1261–1268.
Scholar EM, Violi L and Hexum TD (1987) The antimetastatic activity of enkephalin-like peptides. *Cancer Lett* **35:**133–138.
Sedqi M, Roy S, Ramakrishnan S and Loh HH (1996) Expression cloning of a full-length cDNA encoding delta opioid receptor from mouse thymocytes. *J Neuroimmunol* **65:**167–170.
Simonds WF (1988) The molecular basis of opioid receptor function. *Endocr Rev* **9:**200–212.
Suske G (1999) The Sp-family of transcription factors. *Gene* **238:**291–300.
Vindelov LL and Christensen IJ (1994) Detergent and proteolytic enzyme-based techniques for nuclear isolation and DNA content analysis. *Methods Cell Biol* **41:**219–229.
Zagon IS and McLaughlin PJ (1990) Opioid antagonist (naltrexone) stimulation of cell proliferation in human and animal neuroblastoma and human fibrosarcoma cells in culture. *Neuroscience* **37:**223–226.
Zhu Y, King MA, Schuller AG, Nitsche JF, Reidl M, Elde RP, Unterwald E, Pasternak GW and Pintar JE (1999) Retention of supraspinal delta-like analgesia and loss of morphine tolerance in delta opioid receptor knockout mice. *Neuron* **24:**243–252.

**Address correspondence to:** Dr. Dmitri Smirnov, Department of Pharmacology, University of Minnesota Medical School, 6–120 Jackson Hall, 321 Church Street S.E., Minneapolis, MN. E-mail: smirn001@tc.umn.edu